

International Journal of Radiology and Diagnostic Imaging



E-ISSN: 2664-4444

P-ISSN: 2664-4436

www.radiologypaper.com

IJRDI 2021; 4(2): 132-142

Received: 25-02-2021

Accepted: 27-03-2021

Dr. Gauri Mukhiya

MBBS, MD, Ph.D., Department of Interventional Radiology, The First Affiliated Hospital of Zhengzhou University, Jian she Road Erqi District, Zhengzhou, Henan, China

Dr. Haibao Wang

Professor, MD, Ph.D., Department of Radiology, The First Affiliated Hospital of Anhui Medical University, 218 jixi Road, Hefei, Anhui, China

Dr. Zhili Pan

MD, Ph.D., Department of Radiology, The First Affiliated Hospital of University of Science and Technology of China, Hefei, Anhui

Dr. Longsheng Wang

MD, Ph.D., Department of Radiology, The Second Affiliated Hospital of Anhui Medical University, Hefei, Anhui, China

Dr. Xinwei Han

Professor, MD, Ph.D., Department of Interventional Radiology, The First Affiliated Hospital of Zhengzhou University, Jian she Road Erqi District, Zhengzhou, Henan, China

Dr. Gaurab Pokhrel

MBBS, MD, Ph.D., Department of Interventional Radiology, Zhengzhou University First Affiliated Hospital, Jian she Road Erqi District, Zhengzhou, Henan, China

Dr. Xueliang Zhou

MD, Ph.D., Department of Interventional Radiology, The First Affiliated Hospital of Zhengzhou University, Jian she Road Erqi District, Zhengzhou, Henan, China

Dr. Nighat Parveen

MBBS, MD, Department of Obstetrics and Gynecology, The Third Affiliated Hospital of Zhengzhou University, Zhengzhou, Henan, China

Corresponding Author:

Dr. Xinwei Han

Professor, MD, Ph.D., Department of Interventional Radiology, The First Affiliated Hospital of Zhengzhou University, Jian she Road Erqi District, Zhengzhou, Henan, China

Clinical value of four-quadrant method use in CT and MRI to evaluation of the orbital tumor

Dr. Gauri Mukhiya, Dr. Haibao Wang, Dr. Zhili Pan, Dr. Longsheng Wang, Dr. Xinwei Han, Dr. Gaurab Pokhrel, Dr. Xueliang Zhou and Dr. Nighat Parveen

DOI: <http://dx.doi.org/10.33545/26644436.2021.v4.i2b.209>

Abstract

Purpose: To evaluate the efficacy of four-quadrant method in CT and MRI for diagnosis and differential diagnoses of the orbital tumor. The location of the orbital tumor was assigned to: superolateral, superomedial, inferolateral, inferomedial, and optic nerve were considered as the center point.

Methods: From Sep-2008 to April-2016 a total of 87 cases of orbital tumor were included in study. All included orbital tumors were verified radiologically and histopathologically. Forty nine patients underwent CT scanning and 38 patients underwent MR Imaging. We classified the orbital region according to four-quadrant location method and eight spaces. The frequency distribution of individual CT and MR imaging features in the benign tumor was compared with malignant tumor by using Chi-square tests.

Results: Among the 87 cases of the orbital tumor, 70 cases (80.45%) were benign tumor and 17 cases (19.54%) were malignant tumor. Regarding the four-quadrant location of the orbit, 41 lesions (47.12%) were in superolateral, 18 lesions (20.68%) in inferolateral, 16 lesions (18.39%) in inferomedial, 8 lesions (9.19%) in superomedial, 3 lesions (3.44%) in globe, 1 lesion (1.14%) was in optic nerve. There was significant difference in four quadrant location by comparing benign with malignant tumor ($P=0.023$). Hemangiomas were the predominant benign lesion and lymphoma was major type of malignancy.

Conclusion: The four-quadrant and eight-space (FQES) division of the orbit may play an important role in determining the anatomical location, origin and nature of orbital tumor, and aid in diagnosis and treatment.

Keywords: orbital tumor, four quadrant method; CT; MRI

Introduction

The orbit a small compartment in the skull but may harbor different type of tumors that may be primary and secondary tumor or metastatic in origin. Orbital tumor is most common cause of blindness but has low incidence of diagnosis. An early diagnosis with CT and MRI may prevent chronic eye diseases and blindness. Two third of the orbital tumors is benign and one third of malignant tumors occur in the orbit [1]. The orbital tumor has low incidence of diagnosis and there have several complications after treatment or operation such as cosmetic problems, severe ophthalmological deficit with loss of vision and eye movement [2]. Careful pre-therapeutic work-up for orbital tumor is important to reduce postoperative complications [3-5]. Localizing orbital lesions in relation to specific compartments plays a vital role in the diagnosis and management of these lesions. Tumors are classified according to the site of their origin; inside and outside of the orbit [6]. Computed tomography (CT) and magnetic resonance imaging (MRI) are commonly used imaging modality for characterization of the orbital tumors [7, 8]. Extraconal and intraconal (muscleconal division) spaces only indicated outside and inside of the extraocular muscles, it cannot define exact location such as superior, inferior, superolateral or inferolateral. However, when used four quadrant methods, it can provide exact anatomical location in orbit. Therefore, four quadrant methods may effective in evaluation of orbital soft tissue masses.

The purpose of this study is to demonstrate the significance of four quadrant location used in CT and MRI to evaluate of the orbital tumor for diagnosis and differential diagnosis.

The location of the orbital tumor was assigned to: superolateral, superomedial, inferolateral, inferomedial, and optic nerve were considered as the center point. In addition, we mention 8 spaces; 4 spaces in anterior part and 4 spaces in posterior part of the orbit.

Martial and Methods

General information

From September 2008 to April 2016, we retrospectively analyzed eighty-seven patients with orbital tumors. CT and MRI records from the First Affiliated Hospital, Second Affiliated Hospital and Provincial Hospital were retrieved. All of which were verified on the basics of characteristic finding of CT & MRI and by histopathological diagnosis.

CT and MRI

Orbital CT was performed in 49 patients; a 64 slice MDCT scanner (GE light speed VCT, American) was used. The imaging parameters included: Voltage 120Kvp, tube current 200 mA to 400 mA, helical scan with pitch ratio, 1.375:1, collimation thickness 0.625 × 64 and slice thickness 33mm, Matrix 512 × 512. All CT images were reconstructed by using both a soft tissue algorithm and a bone algorithm. These images were examined in soft tissue window setting (window width = 400 HU and window Level = 40 HU) and in a bone window setting (window width = 2000HU and window level = 200HU) respectively. The iodine contrast agent was injected at a rate of 2.5 ml/sec.

Orbital MRI was performed in 38 patients; 3T MRI (GE, sigma HDxt, America) was used. The parameters were classified as: T1WI FSE sequence (TR: 720 to 1972ms, and TE: 12.0 to 21.9 ms) and T2WI FSE sequence (TR: 4480 to 8571ms, and TE: 95.0 to 119.6ms). A contrast enhanced imaging obtained with T1WI LAVA (TE: 1.2 to 2.6ms,) or 3DBRAVO (TR = 7.8 ms, TE = 3.0ms), Matrix = 256 × 256, FOV = 20 X 20 cm, thickness = 3mm and gap = 0.5cm. The Gd-DTPA was injected at a rate of 2 to 3 mL/sec.

CT and MR imaging evaluation and orbital division Method

The patients underwent either CT or MRI or both. The orbit were divided into four quadrants; superolateral, superomedial, inferolateral, and inferomedial, whereby optic nerve was considered as the centre point. For each tumor, the location, shape, margin, size, density with HU, signal intensity of T1WI and T2WI, enhancement pattern and infiltrative adjustment tissues were analyzed.

Axial section

In the axial section image of MRI, the orbital septum was divided into anterior and posterior part of the orbit (Fig. 1a and 1d).

The posterior part of orbit

In the coronal section image of MRI, optic nerve was considered the center point of the four quadrants. Further to determine and estimate the location of the orbital tumor the compartment was divided by vertical and horizontal axis lines namely; superiolateral, superomedial, inferomedial and inferolateral (Fig. 1b).

Periorbital (anterior part) of orbit

In the coronal section image of MRI, the anterior part of the orbit was divided into four quadrants by vertical and

horizontal axis lines namely; superiolateral, superomedial, inferomedial and inferolateral (Fig. 1c).

Statistical analysis

The data analysis was performed using statistical package for social science (SPSS) Version 16.0 (SPSS, Chicago, IL). The frequency distribution of individual CT and MR imaging features in the benign tumor was compared with malignant tumor by using Chi-square tests. *P* value of less than 0.05 was considered to represent a significant difference.

Results

The orbital tumors were histopathologically confirmed in all 87 patients (43 male and 44 female mean age 47.63 years; range 1-84 years). Benign tumor was diagnosed in 70 patients; of them 34 were male and 36 were female, and the mean age was 45.19 years. Malignant tumor was diagnosed in 17 patients; of them 10 and 7 were male and female with a mean age was 57.71 years. There was no significant difference in the age of patients with benign versus malignant tumors (*P*=0.505) Table 5.3. Similarly, no significant difference was observed in gender when compared patients with benign versus malignant tumors (*P*=0.448) Table 5.4. Thirty six benign tumors and 11 malignant tumors was found in right orbit and 34 benign tumors and 6 malignant tumors found in the left orbit with no significant between the two side regarding benign and malignant tumor (*P*=0.324) Table 5.5. Hemangiomas were the predominant benign lesion and lymphoma was major type of malignancy Table 1.

The orbital tumors' size ranged from 0.8 mm × 4.5 cm to 4.5 cm × 2.0 cm in CT. In 49 cases from CT findings; 23 cases (23/49) had irregular shaped, 13 cases (13/49) had oval shaped, 8 cases (8/49) had round shape, and 5 cases (5/49) had regular shape. Specifically, 32 cases (32/49) were observed with well defined margin and 17 cases (17/49) ill defined margin Table 2. The tumors size ranged from 0.7 cm X 1.2cm X 0.6 cm to 4.0 X 3.5 cm X 2.5 cm, in MRI imaging. Among 38 cases, 14 cases (14/38) were irregular shaped, 12 cases (12/38) were round, 8 (8/38) were oval, 4 (4/38) were regular, 32 had (32/38) well defined margin, and 6 had (6/38) ill defined margin Table 2.

Four quadrants location of the orbit; 41 (47.12%) tumors were located in superolateral part of the orbit, 18 (20.68%) tumors in inferolateral, 16 (18.39%) tumors in inferomedial, 8 (9.19%) tumors in superomedial, 3 (3.44%) tumors in globe and 1 tumor in centre of quadrant Table 3. There was significant difference in four quadrant locations when compared with benign versus malignant tumor (*P*=0.023) Table 5.1. There was also showed significant difference between the lateral and medial side of the orbit in hemangioma and pleomorphic adenoma (*P*=0.027) Table 5.6.

Regarding the anterior and posterior part of the orbit; 56 (64.36%) tumors were located in posterior part, and 31 (35.63%) tumors were located in anterior part. Furthermore, 46 (65.7%) benign tumors and 10 (58.8%) malignant tumors were in posterior part. Twenty four (34.4%) benign tumors and 7 (41.2%) had malignant tumors were in anterior part Table 4. There was no significant difference in anterior and posterior region for benign versus malignant tumor (*P*=0.675) Table 5.2.

Discussion

To our knowledge, the present study represented the first retrospective study for four quadrant methods used in CT and MRI to evaluate diagnosis and differential diagnosis of orbital tumor. We found a significant difference in four quadrant location of the orbit for benign versus malignant tumors. Most of the benign and malignant tumors were located in superolateral quadrant. Significant differences between the lateral and medial side of the orbit was seen with majority of tumors located in lateral side. Moreover, most of the malignant tumors were located in lateral side of the orbit.

There was no significant difference in the age and sex of patients between benign versus malignant tumor. In line with our findings, a previous study found no significant difference in the age and sex of patients with benign versus malignant tumor. The same study reported no significant difference in the side involvement of tumors between the benign versus malignant tumor^[9]. The age of the patients in our study was divided into two groups, group A (0-30 years) and group B (>30 years). Orbital tumor was more common in group B and malignant tumor was also prominent in the same group Table 5.3. The incidence of orbital tumors was relatively low in group A and higher in group B.

Most of the benign and malignant tumors were located in superolateral quadrant and malignant tumors were related with lacrimal gland. The cavernous hemangioma was found in all four quadrants, but was predominant in the inferolateral quadrant. Our findings were similar to previous studies^[10-12]. Most of the pleomorphic adenoma, dermoid cyst, lymphoma, adenoid cystic carcinoma and inflammatory pseudotumor, solitary fibrous tumors were located in the superolateral quadrant. The retinoblastoma and choroidal melanoma were localized in the globe and while meningioma was found in central point in orbit.

Four quadrant methods in CT and MRI imaging feature can effectively distinguish between benign and malignant orbital tumor. The study showed that most of the malignant tumors had ill-defined margins, irregular shape, infiltrative adjustment of tissues and bone erosion, iso/slightly high density, low intensity on T1WI, iso/slightly high intensity on T2WI and heterogeneous enhancement. Most of the benign tumors had well defined margin, oval/round shape, isodensity, low intensity on T1WI, high or slightly intensity on T2WI and homogeneous enhancement. The radiological finding was supported by previously described^[9]. It was previously documented that CT and MRI images are important modalities in diagnosis and assessment of the location and extent of a pathological process prior to

surgical exploration and others differential diagnosis^[11, 13].

This study showed that cavernous hemangioma was found in all four quadrants, but more seen in the inferolateral quadrant and it had well defined margin, oval/round shape, intraconal space^[14], slightly high density, low signal intensity on T1WI, high signal intensity on T2WI and gradual homogeneous enhancement (Fig. 2). These findings are similar with previous studies^[12, 15, 16].

Pleomorphic adenoma showed regular/oval shape well defined, mixed isodensity and mixed heterogeneous enhancement (Fig. 3) and irregular shaped, ill defined, isodensity, slightly heterogeneous enhancement and infiltrative adjustment tissues and bone erosion in adenoid cystic carcinoma. Our findings are similar with previous studies^[17]. They were frequently seen in the superolateral, extraconal space and between the globe and orbital periosteum^[18]. The CT and MRI findings are key to define the differential diagnosis of dermoid and epidermoid cyst with others benign and malignant tumors of the orbit. CT and MRI showed a well circumscribed cystic tumor of the low or fat density with calcification (Fig. 4) and typically appeared hyperintense on T1WI and hypointense on T2WI. The orbital lymphoma usually infiltrates structures in superolateral quadrant with frequent involvement of superior and lateral rectus muscles (Fig. 5). The orbital malignant lymphoma usually manifests as a diffuse solid, enhancing mass with molding around the globe on images studies, and reflecting the irregular infiltrative of orbital structures^[19, 20]. The orbital pseudotumor is benign tumor in the orbit and it mostly located in superolateral and inferolateral quadrant (Fig. 6). Orbital lymphoma can be very difficult to distinguish from orbital pseudotumor, however the lymphoma is usually seen with decreased density on delayed images in dual-phase-spiral CT contrast, and orbital pseudotumor is mostly seen with increased density on delayed images in dual-phase CT contrast^[21].

The four quadrant location and eight spaces are not only for guided to diagnosis and differential diagnosis. It can determine the accurate description of tumor location and involved adjustment tissues surrounding lesion, may facilitate proper treatment planning. Extraconal and intraconal (muscleconal division) spaces only indicated outside and inside of the extraocular muscles, it cannot define exact location such as superior, inferior, superolateral or inferolateral. However, when used four quadrant methods, it can provide superior, inferior, medial, lateral and exact anatomical location in orbit so, may have comparatively easier to diagnosis and differential diagnosis in orbital tumor.

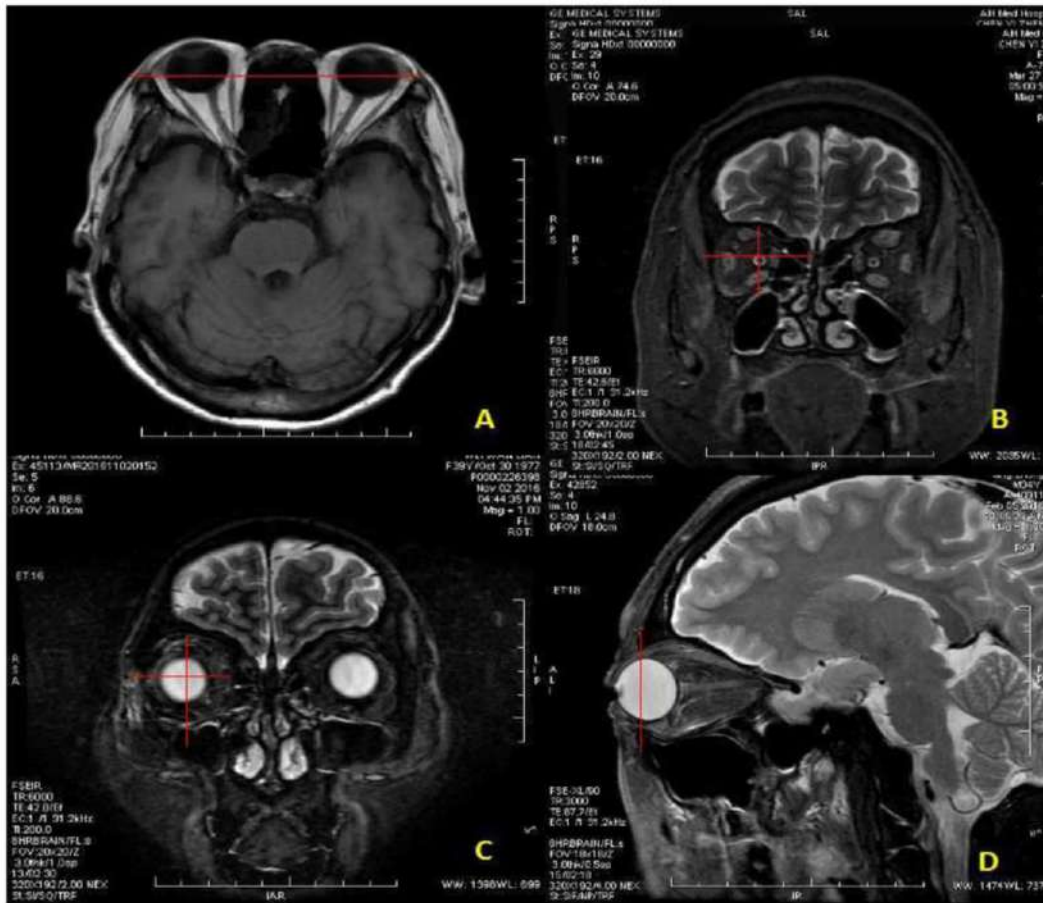


Fig 1a: the orbital septum was used for differentiated location of anterior and posterior part of orbit. **Fig 1b** The posterior part of the lesion was positioned with optic nerve in coronal section image. **Fig 1c:** The anterior part lesion around the globe was positioned with annulus of eye in center of coronal section image. **Fig.1d** The orbital septum was used for anterior and posterior part of lesion on sagittal section image.

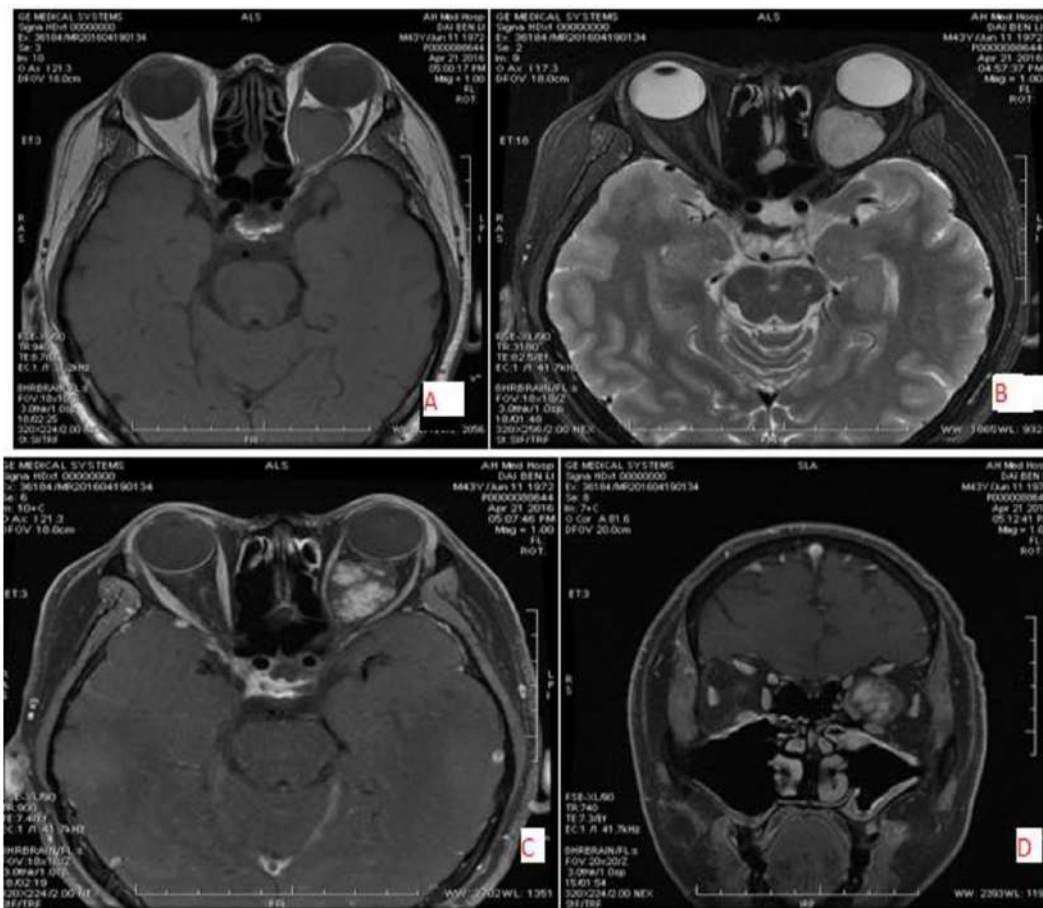
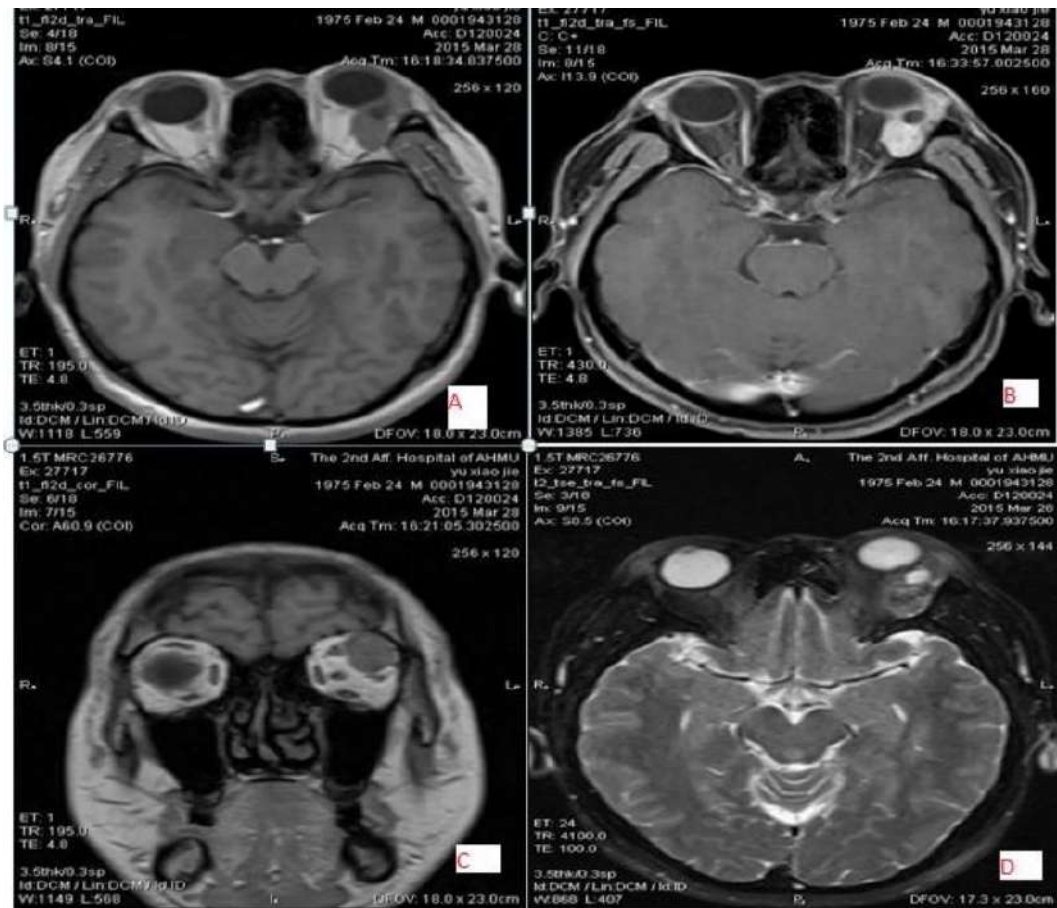




Fig 2: 44 years old male with left sided cavernous hemangioma, located in intraconal and superomedial region with oval shape and well defined, low signal intensity on T1WI(A) and high signal intensity on T2WI (B) and gradual homogeneous enhancement (C&D) and 44years old female patient with right sided schwannoma, located in intraconal and inferolateral region with well define margin and oval shaped, low signal intensity on T1WI (A) and slightly high signal intensity on T2WI(B&C) and marked homogeneous enhancement (D).



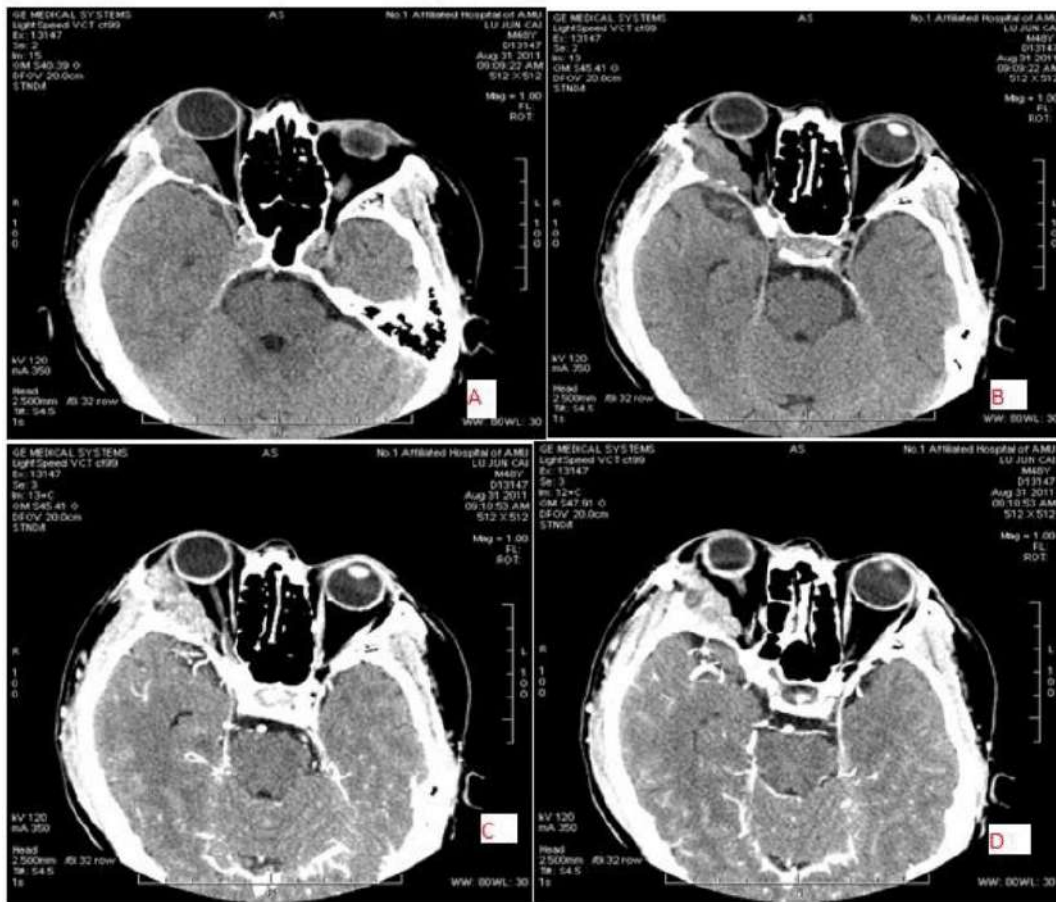


Fig 3: 40 years old male with left sided pleomorphic adenoma, located in extraconal and superiolateral region with irregular shaped and ill defined, mixed signal intensity on T1WI (A) and mixed signal intensity on T2WI (D) and marked homogeneous enhancement (B&C) and 47 years old male with Right sided pleomorphic adenoma, located extraconal and superiolateral region with irregular shaped and ill defined, mixed density (30-40 HU) (A&B) and mixed heterogeneous enhancement (C&D).

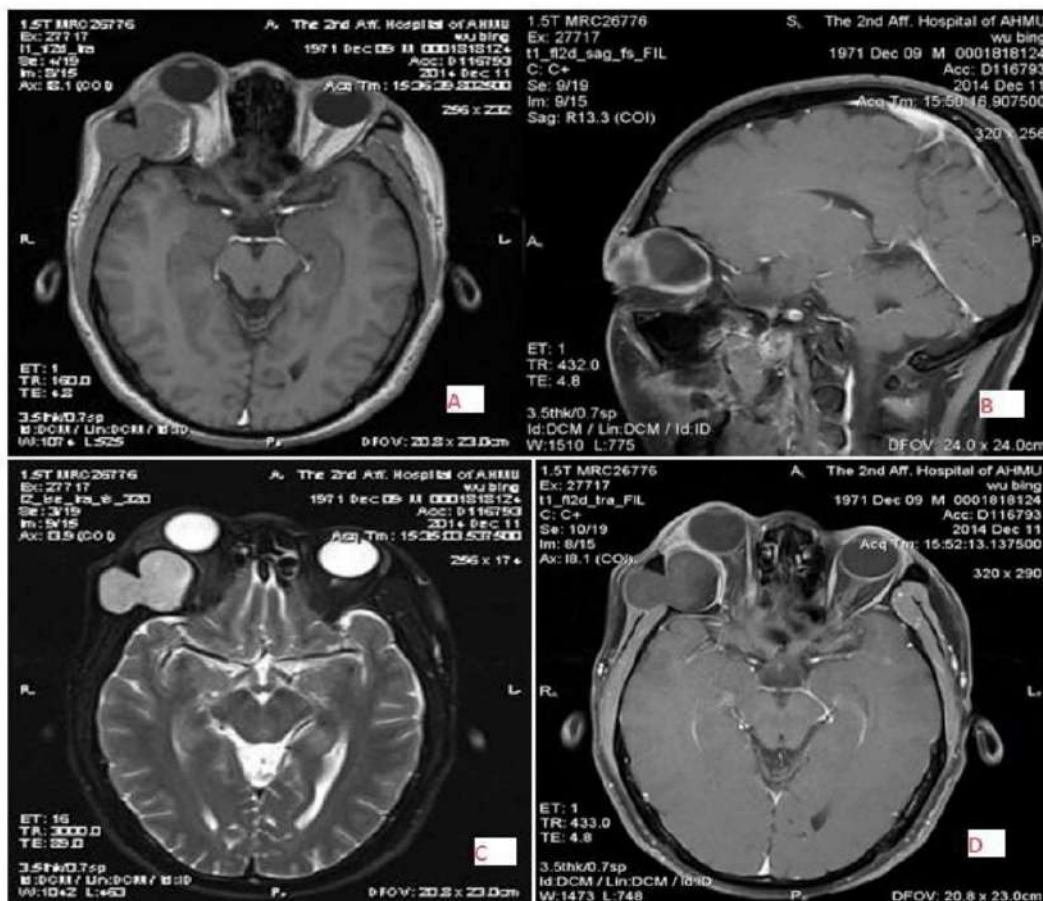
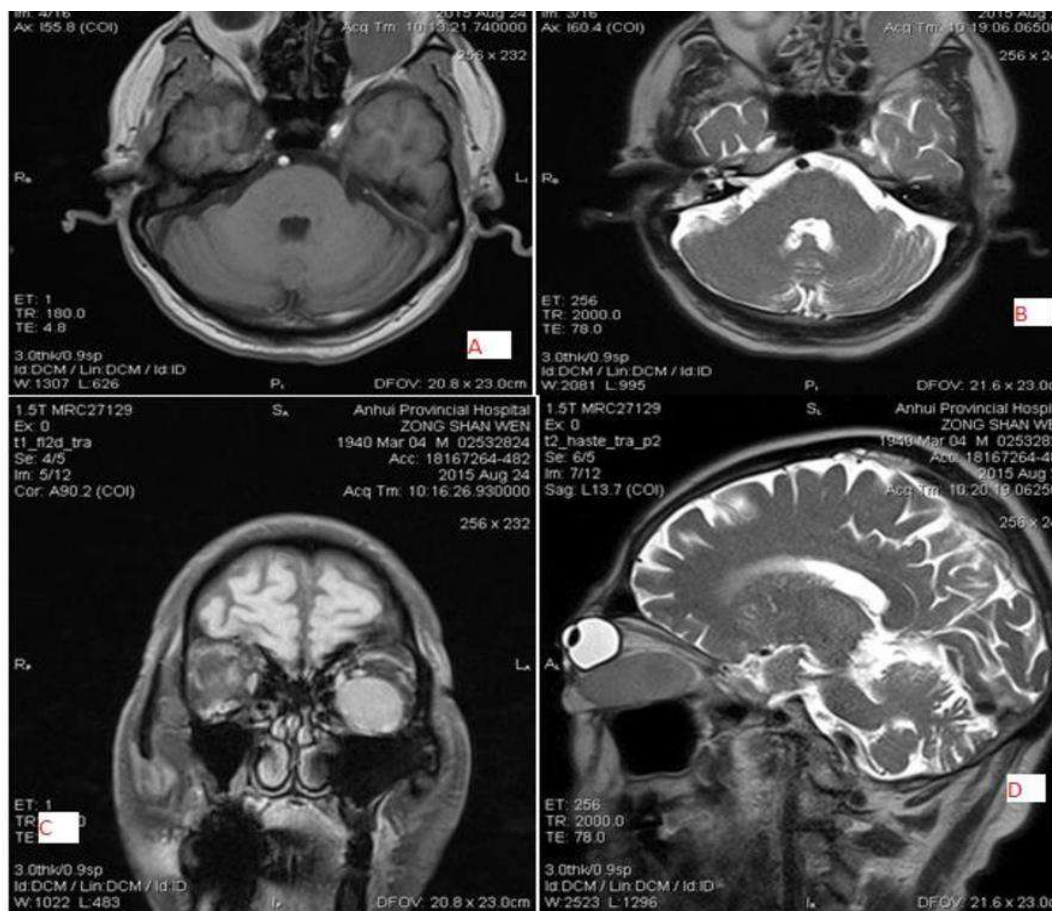




Fig 4: 43 years old male with Right sided dermoid cyst located in extraconal and superiolateral region with irregular mass and well defined, slightly low signal intensity On T1WI (A) and slightly high signal intensity on T2WI(C) and Boundary homogeneous enhancement(B&D) and 64 years old female with left sided dermoid cyst, located in extraconal and inferomedial region with regular shaped and well defined, iso-density (40 HU)[A, B, C, & D].



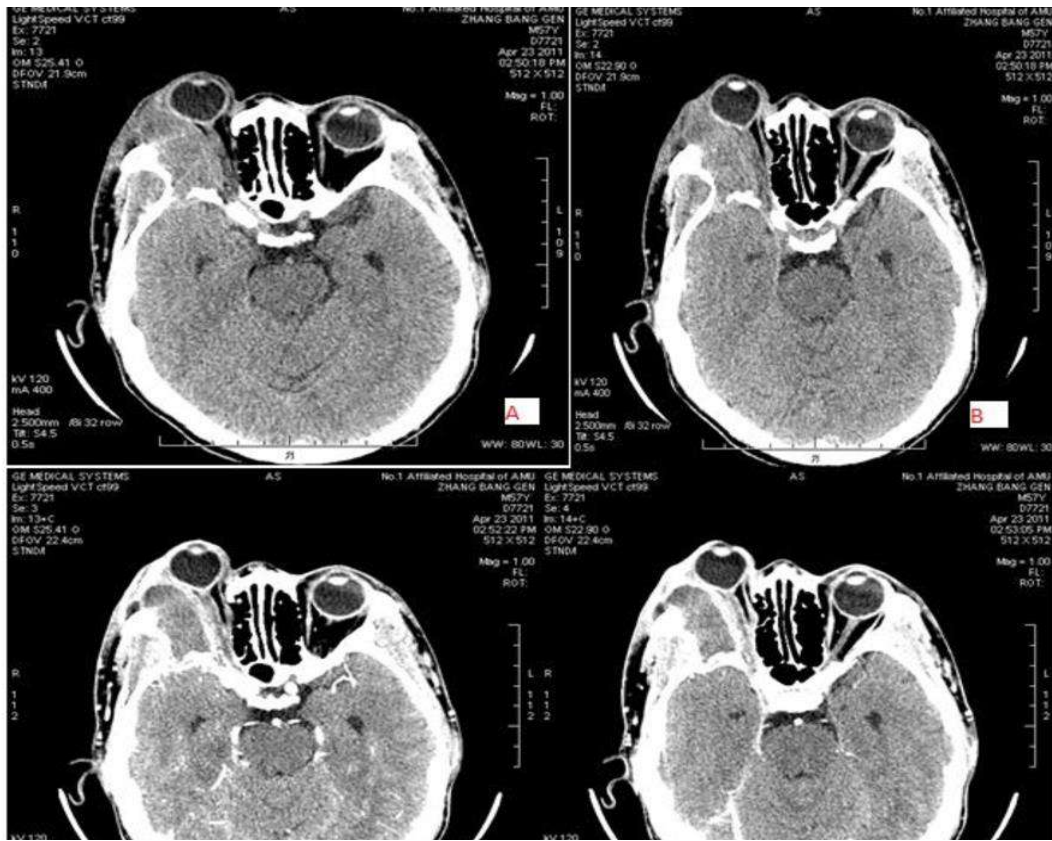


Fig 5: 75 years old male with left sided lymphoma, located in extraconal and inferomedial region with regular shaped and well margin, slightly low signal intensity on T2WI (A) and iso intensity on T2WI (B & D) and marked homogeneous enhancement (C) and 57 year old male with right sided lymphoma, located in extraconal and superolateral region with irregular mass and ill defined with invaded bone, iso density (38 HU) [A&B] and slightly homogeneous enhancement (C&D).

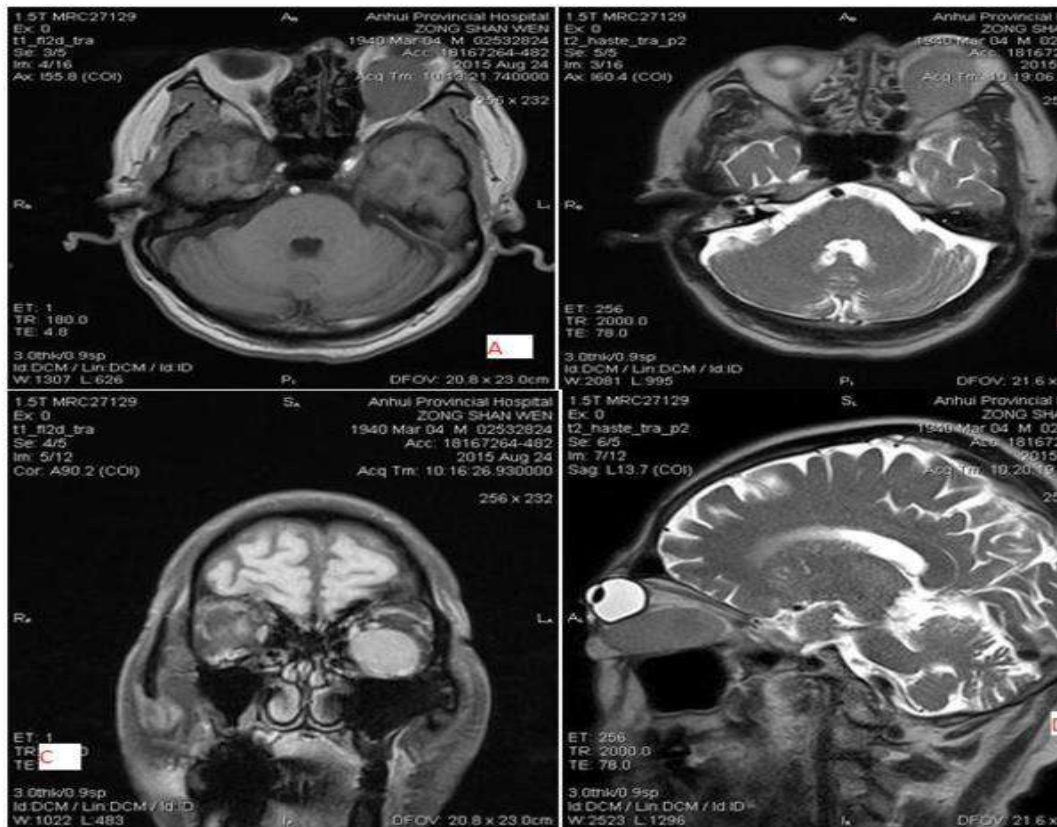


Fig 6: 39 years old female with left sided Inflammatory pseudotumor, located in extraconal and inferolateral region with irregular shaped and well margin, low signal intensity on T1WI (A) and slightly high signal intensity on T2WI (B&D) and mixed with intermeditated enhancement (C) and 75 years old male with left sided lymphoma, located in extraconal and inferomedial region with regular shaped and well margin, slightly low signal intensity on T2WI (A) and iso intensity on T2WI (B & D) and marked homogeneous enhancement (C).

Table 1: Constitutions ratio of orbital tumor

S/N	Name	Case of number	Percent
1	Hemangioma	36	41.37%
2	Pleomorphic adenoma	9	10.34%
3	Dermoid cyst	9	10.34%
4	Lymphoma	7	8.04%
5	Infla. pseudotumor	5	5.74%
6	Adenoid cystic carcinoma	3	3.44%
7	Solitary fibrous tumor	3	3.44%
8	Lipoma	3	3.44%
9	Choroidal melanoma	2	2.29%
10	Retinoblastoma	1	1.14%
11	Malignant melanoma	1	1.14%
12	Dedifferentiated chondrosarcoma	1	1.14%
13	Metastasis	1	1.14%
14	Meningioma	1	1.14%
15	Schwannomas	1	1.14%
16	Granulomatous inflammation	1	1.14%
17	Lymphangiomyoma	1	1.14%
18	Squamous cell carcinoma	1	1.14%
19	Cystadenoma	1	1.14%
	Total	87	100%

S/N serial number, Infla. = inflammation

Table 2: CT and MRI - Imaging Finding of orbital tumor

Features	CT (Total=49)	MRI (Total=38)
1. Size range	0.8 mm × 4.5 cm to 4.5 cm × 2.0 cm	0.7 cm x 1.2cm x 0.6 cm to 4.0 x 3.5 cm x 2.5 cm
2.Shape		
- Irregular	23	14
-Regular	5	4
- Oval	13	8
-Round	8	12
3.Margin		
- well defined	32	32
- ill defined	17	6
4.Hunsfield Unit		
- Non- Contrast(range)	12 to 122	-
- Contrast (range)	52 to 85	-
5.Density		
-Iso	22	-
-Slight high	15	-
-Mixed	6	-
- Low	5	-
-High	1	-
6. Intensity	-----	most of the cases were hypo-intensity on T1WI and hyper-intensity on T2WI
7.Pattern of Contrast		
-Gradual homogeneous	-	14
-Gradual heterogeneous	-	1
- Marked homogeneous	3	7
- Marked heterogeneous	2	4
-Slightly homogeneous	7	1
- Slightly heterogeneous	3	-
-Mixed heterogeneous	2	2
-Focal heterogeneous	1	-
- Intermediate homogeneous	-	3
- intermediate heterogeneous	-	-
- Boundary heterogeneous	-	3
8.Non- Contrast	31	3
9.Infiltrative adjustment tissues	8	5

Table 3: Distribution of orbital tumor in four quadrants

S/N	Name	Number Of case	Sup/med	Sup/lat	Infero/med	Infero/lat	Globe	Optic nerve
1	Hemangioma	36	7	9	8	12	0	0
2	Pleomorphic adenoma	9	0	9	0	0	0	0
3	Dermoid cyst	9	0	7	2	0	0	0
4	Lymphoma	7	0	3	2	2	0	0
5	Infla. Pseudotumor	5	0	4	0	1	0	0
6	Adenoid cystic carcinoma	3	0	3	0	0	0	0
7	Solitary fibrosis tumor	3	0	2	1	0	0	0
8	Lipoma	3	1	1	0	1	0	0
9	Choroidal melanoma	2	0	0	0	0	2	0
10	Metastasis	1	0	0	0	1	0	0
11	Meningioma	1	0	0	0	0	0	1
12	Malignant melanoma	1	0	0	1	0	0	0
13	Retinoblastoma	1	0	0	0	0	1	0
14	Dedi-Chondrosarcoma	1	0	0	0	1	0	0
15	Schwannomas	1	0	0	1	0	0	0
16	Granulomatous infla.	1	0	0	1	0	0	0
17	Lymphangiomyoma	1	0	1	0	0	0	0
18	Squamous cell carcinoma	1	0	1	0	0	0	0
19	Cystadenoma	1	0	1	0	0	0	0
	Total	87	8	41	16	18	3	1

S/N = serial number, sup/med = superomedial, sup/lat = superolateral, infero/med= inferomedial, infero/lat =inferomedial, Dedi= dedifferentiated

Table 4: Distribution of orbital tumors in anterior, posterior part, extraconal and intraconal

Name	Anterior	Posterior	Extraconal	Intraconal	Globe
Hemangioma	7	29	11	25	
Pleomorphic adenoma	7	2	9	0	
Dermoid cyst	6	3	9	0	
Lymphoma	3	4	7	0	
Infla. pseudotumor	2	3	5	0	
Adenoid cystic carcinoma	3	0	3	0	
Solitary fibrous tumor	2	1	3	0	
Lipoma	0	3	2	1	
Choroidal melanoma	0	2	0	0	2
Retinoblastoma	0	1	0	0	1
Malignant melanoma	1	0	1	0	
Dedifferentiated chondrosarcoma	0	1	1	0	
Metastasis	0	1	0	1	
Meningioma	0	1	0	1	
Schwannomas	0	1	0	1	
Granulomatous inflammation	0	1	1	0	
Lymphangiomyoma	0	1	1	0	
Squamous cell carcinoma	0	1	1	0	
Cystadenoma	0	1	0	1	
Total	31	56	54	30	3

Table 5: Benign tumor versus malignant Tumor

5.1: Significant different in four quadrant location of benign tumor versus malignant Tumor

Location	Benign tumor	Malignant	Total	P - value
Superolateral	32 (45.7%)	6 (35.3%)	43.7%	
Superomedial	9 (12.9%)	2 (11.8%)	12.6%	0.023
inferolateral	15 (21.4%)	3 (17.6%)	20.7%	
Inferomedial	13 (18.6%)	3 (17.6%)	18.4%	
In globe	0 (0.0%)	3 (17.6%)	3.4%	
In optic never	1 (1.4%)	0.0%	1.1%	

5.2: Significant different in Anterior and Posterior part of orbit for benign versus malignant tumor

Orbit	Benign tumor	Malignant tumor	P -value
Anterior	24 (34.2%)	7 (41.2%)	0.675
Posterior	46 (65.7%)	10 (58.8%)	

5.3: Benign versus malignant tumors of Age Groups

Age Group	Benign tumor	Malignant tumor	P - value

0-30	13 (18.6%)	2 (11.8%)	0.505
>30	57 (81.5%)	15 (88.2%)	
5.4: Benign versus malignant tumor of Sex of patients			
Sex	Benign tumor	Malignant tumor	P-value
Male	34 (48.6%)	10 (58.8%)	0.448
Female	36 (51.4%)	7 (41.2%)	
5.5: Benign versus malignant tumor of Side of Eye			
Side of eye	Benign tumor	Malignant tumor	P- value
Right	36 (51.4%)	11 (64.7%)	0.324
Left	34 (48.6%)	6 (35.3%)	

5.6: A Comparison of the spatial distribution between cavernous hemangioma and pleomorphic adenoma						
	Location	Hemangioma	Pleomorphic adenoma	Total	X ²	P-value
Medial	superomedial	7	1		10.28	0.027
	Inferomedial	8	-			
		15	1	16		
Lateral	superiolateral	9	7			
	inferolateral	12	1			
		21	8	29		

Conclusion

This data indicate that the four-quadrant and eight-space (FQES) division of the orbit may play an important role in determining the anatomical location, origin and nature of orbital tumor, and aid in diagnosis and treatment. It has supplementary role to traditional muscleconal division in the assessment of the orbital tumors.

References

- Shields JA, Shields CL, Scartozzi R. Survey of 1264 patients with orbital tumors and simulating lesions: The 2002 Montgomery Lecture, part 1. *Ophthalmology*. 2004;111(5):997-1008.
- Ohtsuka K, Hashimoto M, Suzuki Y. A review of 244 orbital tumors in Japanese patients during a 21-year period: origins and locations. *Jpn J Ophthalmol*. 2005;49(1):49-55.
- Demirci H, Shields CL, Shields JA, *et al*. Orbital tumors in the older adult population. *Ophthalmology* 2002;109(2):243-8.
- Moss HM. Expanding lesions of the orbit. A clinical study of 230 consecutive cases. *Am J Ophthalmol*. 1962;54:761-70.
- Shields JA, Bakewell B, Augsburger JJ *et al*. Classification and incidence of space-occupying lesions of the orbit. A survey of 645 biopsies. *Arch Ophthalmol* 1984;102(11):1606-11.
- Armington WG, Bilaniuk LT. The radiologic evaluation of the orbit: conal and intraconal lesions. *Semin Ultrasound CT MR* 1988;9(6):455-73.
- Aviv RI, Miszkiel K. Orbital imaging: Part 2. Intraorbital pathology. *Clin Radiol* 2005;60(3):288-307.
- Lemke AJ, Kazi I, Felix R. Magnetic resonance imaging of orbital tumors. *Eur Radiol*. 2006;16(10):2207-19.
- Xian J, Zhang Z, Wang Z *et al*. Value of MR imaging in the differentiation of benign and malignant orbital tumors in adults. *Eur Radiol*. 2010;20(7):1692-702.
- Ansari S, Mafee M. Orbital Cavernous Hemangioma: Role of Imaging. *Neuroimaging clinics of North America*. 2005;15:137-58.
- Berletti R, Cavagna E, Cimini N *et al*. Dissection of epiaortic vessels: clinical appearance and potentiality of imaging techniques. *Radiol Med*. 2004;107(1-2):35-46.
- Xian J, Zhang Z, Wang Z, *et al*. Evaluation of MR

- imaging findings differentiating cavernous haemangiomas from schwannomas in the orbit. *Eur Radiol* 2010;20(9):2221-8.
- Weber AL, Sabates NR. Survey of CT and MR imaging of the orbit. *Eur J Radiol* 1996;22(1):42-52.
- Ansari SA, Mafee MF. Orbital cavernous hemangioma: role of imaging. *Neuroimaging Clin N Am*. 2005;15(1):137-58.
- Fries PD, Char DH, Norman D. MR imaging of orbital cavernous hemangioma. *J Comput Assist Tomogr*. 1987;11(3):418-21.
- Forbes G. Vascular lesions in the orbit. *Neuroimaging Clin N Am* 1996;6(1):113-22.
- Mafee MF, Haik BG. Lacrimal gland and fossa lesions: role of computed tomography. *Radiol Clin North Am*. 1987;25(4):767-79.
- Mafee MF, Edward DP, Koeller KK *et al*. Lacrimal gland tumors and simulating lesions. Clinicopathologic and MR imaging features. *Radiol Clin North Am*. 1999;37(1):219-39, xii.
- Demirci H, Shields CL, Karatza EC *et al*. Orbital lymphoproliferative tumors: analysis of clinical features and systemic involvement in 160 cases. *Ophthalmology* 2008;115(9):1626-31, 1631.e1-3.
- Sullivan TJ, Valenzuela AA. Imaging features of ocular adnexal lymphoproliferative disease. *Eye (Lond)*. 2006;20(10):1189-95.
- Moon WJ, Na DG, Ryoo JW *et al*. Orbital lymphoma and subacute or chronic inflammatory pseudotumor: differentiation with two-phase helical computed tomography. *J Comput Assist Tomogr* 2003;27(4):510-6.